PCCP

Accepted Manuscript

ROYAL SOCIETY OF CHEMISTRY

www.rsc.org/pccp

Journal Name

ARTICLE

Combined experimental and density functional theory studies of an Organic-inorganic hybrid perovskite

Received 00th January 20xx,
Accepted 00th January 20xx

DOI: 10.1039/x0xx00000x

www.rsc.org/

S. Kassou,[a] R. El-Mrabet,[a] A. Kaiba,[c] P. Guionneau,[b] and A. Belaaraj [a]

Single crystals of $[C_6H_5\text{-}C_2H_4\text{-}NH_3]_2ZnCl_4$ were obtained by slow evaporation at room temperature. Single-Crystal X-Ray Diffraction (SCXRD), Differential Scanning Calorimetry (DSC), Thermogravimetric Analysis (TGA) and UV-Visible spectroscopy were used to characterize the crystal structure, thermal and optical properties respectively. At 293 K PEA-$ZnCl_4$ crystallizes in a monoclinic unit-cell, $P2_1/c$ space group (a=7.449(2) Å, b=24.670(3) Å, c=11.187(2) Å and β= 91.762(5)°, V=2054.8 (2) $Å^3$ and Z=4. The DSC and TGA analysis show respectively the presence of two first order reversible phase transitions and a sample thermal stability below 541 K. The optical study reveals that the compound undergoes a direct optical transition and an energy gap about of Eg= 4.46 eV. In parallel, an ab-initio DFT calculation is performed to study the electronic band structure, to examine electronic density and to calculate the gap energy value. The calculated values are in good agreement with the experimental data.

Introduction

Organic-inorganic hybrids perovskite have drawn increasing interest notably from both the experimental and theoretical scientific communities for the past decades due to their interesting structure, optical, thermal properties [1-11] and their promising applications in many areas like optoelectronic devices, magnetic and solar cell [12-14]. Their structure consists of alternating layers between organic and inorganic moieties and they have new properties intermediate between those of the two constituent moieties [15, 16]. The optical properties like band gap present one of the interesting features of this kind of compounds. They constructs a multi-quantum well energy band [1, 15]: the inorganic anion constructs the well deep of the multiple quantum wells because the energy bands near of the Fermi level is mainly governed by the orbital of inorganic atoms [17], while the organic cation plays the role of a potential barrier, this lead to a new kind of functional material [18]. In this regard there is certain interest focus the compounds based on $ZnCl_4^{2-}$ for its lower dimensionality (0 D), solid–solid phase transformation, and Alternative current conduction and for their Ferroelectric properties[19-22]. The correlation between the electronic structure and macroscopic properties (eg gap energy and density of state) can benefit from predictive modelling of these materials using density functional theory (DFT).

In the present work, we report for $[C_6H_5\text{-}C_2H_4\text{-}NH_3]_2ZnCl_4$ (hereinafter PEA-$ZnCl_4$), synthesis, crystal structure, phase transition temperature, enthalpy and entropy determined by Differential Scanning Calorimetry (DSC) and weight loss by Thermogravimetric analysis (TGA). The optical band gap energy for PEA-ZnCl4 is determined by UV-Visible spectroscopy and was compared to the value obtained from DFT calculation. The band structure and density of state were also calculated.

Experimental

Crystal growth

The single crystals of the $(C_6H_5\text{-}C_2H_4\text{-}NH_3)_2ZnCl_4$ compound hereinafter called as PEA-$ZnCl_4$ were grown by slow evaporation of the concentrated aqueous solution at room temperature. The typical experimental process is as follows: 560 mg (1 mmol) of $ZnCl_2$ was dissolved in 5 ml of water. In other hand we have dissolved 0.5 ml of phenylethylamonium (1 mmol) in 7 ml of ethanol/water (1:1 in ratio) protonated by few drops of HCl (37 %). The mixture between these solutions was carried out at room temperature in a glass tube. White plate-like crystals were obtained after several weeks.

[a] *Laboratoire de Physique des matériaux et modélisation des Systèmes (LP2MS), Unité Associée au CNRST-URAC 08, Faculté des Sciences, Université Moulay Ismail, B.P. 11201, Zitoune, Meknès, Morocco.*
[b] CNRS, Univ. Bordeaux, ICMCB, UPR 9048, F-33600 Pessac, France.
[c] *Physic Department, College of Sciences and Humanities, Prince Sattam bin Abdulaziz University, P.O. Box 83,Al-Kharj11942, Saudi Arabia.*

E-mail : a.belaaraj@fs-umi.ac.ma

Crystallographic characterization

A PEA-$ZnCl_4$ crystal was selected under a polarizing microscope in the order to perform its structural analysis by SCXRD. The measurements were performed on a Nonius Kappa CCD with Mo-Kα radiation. The collection was made at room temperature using a mixture of Φ, Ω scan mode. The structure was solved by SIR97 [23] and the refinement of atomic parameters based on full-matrix least squares technique F^2 was performed using SHELX97 [24]. The non-hydrogen atoms were refined anisotropically and the hydrogen atoms were placed theorically. All above programs were used within the WINGX package [25]. The drawings were made with Diamond [26]. The crystallographic data and experimental parameters for the intensity collection are summarized in the Table 1.

Table 1 Crystallographic and structure refinement data for PEA-ZnCl4

Empirical formula	C16 H24 Zn Cl4 N2
Formula weight	451.54
Temperature	293(2) K
Wavelength	0.71073 Å
Crystal system	Monoclinic
Space group	$P2_1/c$
Unit cell parameters	a = 7.449 (2) Å b = 24.670(3) Å c = 11.187(2) Å β = 91.762 (5) °
Volume	2054.8 (2) $Å^3$
Z	4
Density (calculated)	1.46 g/cm^3
Absorption coefficient	1.715 mm^{-1}
F(000)	927.9
Crystal size	0,.3 x 0,.5 x 0,.03 mm^3
Θ range data collection	2.46 ° to 26.37 °
Index ranges	-9 ≤ h ≤ 9 -30 ≤ k ≤ 30 -13 ≤ l ≤ 13
Reflections collected	4186
Independent reflections	3050
Completeness to(Θ)	26.36 °- 99.5 °
Absorption correction	Empirical
Refinement method	F^2 Full-matrix
Data/Restraints/Parameters	4186/210/0
Goodness-of-fit on F2	1.078
Final R indices [I>2 σ(I)]	R1 = 0.0363, wR2 = 0.0925
R indices (all data)	R1 = 0.0431, wR2 = 0.111

Thermal analysis

The Thermogravimetric analysis (TGA) was performed using a DTG-60H Analyzer, from 288 to 530 K on a 16.410 mg of PEA-$ZnCl_4$. A Differential scanning Calorimetry (DSC) measurements were performed using a DSC131 Evo instrument. The measurements were carried out on a 10 mg of PEA-$ZnCl_4$ loated into an enclosed alumina crucible with heating and cooling rates of 5°C/min under nitrogen atmosphere. The crystallization points were determined from the tangential sigmoidal baseline fitting of the endothermic and exothermic peaks, respectively.

UV-vis diffuse reflectance spectrum

The UV-vis diffuse reflectance spectroscopy was performed on a jasco v-570 spectrophotometer over the spectral range 200-1200nm. A barium sulfate ($BaSO_4$) plate was used as the standard (100 % reflectance) on which the finely ground sample from the crystal was coated. The absorption spectrum was calculated from the reflectance spectrum using the Kubelka-Munk function: $F(R) = (1-R)^2/(2R)$ [27] were R is the reflectance.

Computational details

All of the calculations were performed within the framework of (DFT) [28] by using the Perdew, Burke, and Ernzerfhof (PBE) generalized gradient approximation (GGA) with Fritz-Haber-Institute (FHI) pseudopotentials [29] implemented in the ABINIT package [30]. The 4x4x4 k-point meshes are used to perform the Brillouin Zone integrations by considering the Monkhorst Pack scheme [31]. Plane-wave basis set have been chosen with an energy cutoff of $|K+G|^2 \leq 600$ eV and was used in all calculations. The experimental data were used as a starting point for the optimization of atomic positions. The atomic positions within the unit cell relaxed until the forces were less than 0.01 eV/Å, the displacement parameters, between experimental and optimized atomic positions along the tree axis, are shown in Table 2.

Table 2 Displacement (Å) parameters of Zn, Cl, N, C atoms for PEA-$ZnCl_4$

	U_{xx}	U_{yy}	U_{zz}
Zn	**0.002542**	**0.042753**	**0.000980**
Cl	**0.003151**	**0.092835**	**0.002073**
Cl	**0.001404**	**0.108039**	**0.001343**
Cl	**0.001521**	**0.113270**	**0.000471**
Cl	**0.001279**	**0.001980**	**0.003772**
N	**0.033497**	**0.004676**	**0.006924**
N	**0.025188**	**0.006588**	**0.017732**
C	**0.002100**	**0.000500**	**0.000300**
C	**0.000100**	**0.000010**	**0.000900**
C	**0.001400**	**0.000290**	**0.001900**
C	**0.000900**	**0.000600**	**0.000400**
C	**0.001800**	**0.000760**	**0.000200**
C	**0.000600**	**0.000400**	**0.000800**
C	**0.000100**	**0.000380**	**0.002300**
C	**0.000900**	**0.001100**	**0.001800**
C	**0.001300**	**0.000300**	**0.000200**
C	**0.001900**	**0.001200**	**0.000200**
C	**0.005700**	**0.000900**	**0.001700**
C	**0.001900**	**0.001200**	**0.001200**
C	**0.002500**	**0.000000**	**0.000300**
C	**0.000800**	**0.001500**	**0.003000**
C	**0.001800**	**0.000500**	**0.000900**
C	**0.000700**	**0.001100**	**0.002100**

Results and discussion.

Structural description

The PEA-$ZnCl_4$ compound crystallizes in the monoclinic system with $P2_1/c$ space group and the cell parameters a=7.449(5)Å, b=24.670(5)Å, c=11.187(5)Å, β= 91.762(5)°, V=2054.8 (2) $Å^3$ and Z=4. The asymmetric unit is formed by one $[ZnCl_4]^{2-}$ anion and two $(C_6H_5\text{-}C_2H_4\text{-}NH_3)^+$ cations (Figure 1). The Overall structure consists of 0D inorganic network, interplayed by the phenylethylammonium bilayer ions (Figure 2). In the inorganic layer, Zn-Cl distances (2.230(4) to 2.279(3) Å) are shorter compared to similer bromated compound Zn-Br (2.3839(14) to 2.4104(14) Å) for $(C_6H_5\text{-}C_2H_4\text{-}NH_3)_2ZnBr_4$ [32] this is due to the difference in halogen radius, which have effect on tetrahedral geometry. The Baur distortion indices (ID) [33] are calculated for PEA-$ZnCl_4$:

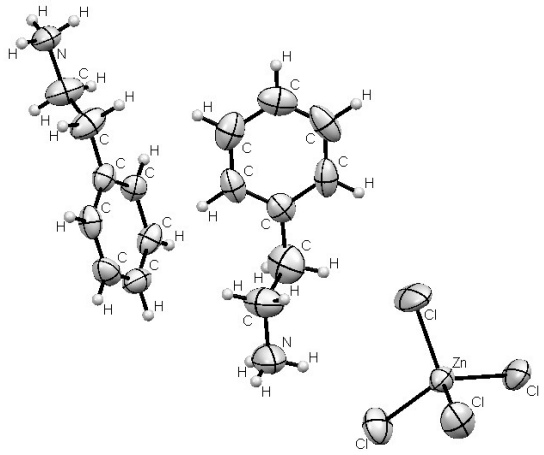

Fig. 1 Asymmetric unit cell of PEA-$ZnCl_4$

The Baur distortion indices (ID)

$$ID(d)=\sum_{i=1}^{4}\frac{|ZnCl_i\text{-}ZnCl_m|}{4(ZnCl_m)}$$

and

$$ID(\varphi)=\sum_{i=1}^{6}\frac{|ClZnCl_i\text{-}ClZnCl_m|}{6(ClZnCl_m)}$$

Where m means the value for the polyhedron, d= Zn-Cl distance and ϕ= Cl-Zn-Cl angle, are calculated for PEA-$ZnCl_4$. The obtained indices (ID(d)= 7.30 . 10^{-3}; ID(ϕ)= 0.011) are slightly lower than that obtained for the similar compounds $(C_8H_{10}NO)_2ZnCl_4$ [34] (ID(d)= 7.63 . 10^{-3}; ID(φ)= 0.019). These values clearly indicate that the $[ZnCl_4]^{-2}$ anion has a slightly distorted tetrahedral stereochemistry.

Table 3 Selected interatomic distances (Å) and angle (°) in the inorganic part

$Zn\text{-}Cl_i$ (Å)	$Cl_j\text{-}Zn\text{-}Cl_k$ (°)
$Zn\text{-}Cl_2$ 2.272 (3)	$Cl_2\text{-}Zn\text{-}Cl_3$ 107.40 (1)
$Zn\text{-}Cl_3$ 2.279 (3)	$Cl_3\text{-}Zn\text{-}Cl_4$ 110.66 (1)
$Zn\text{-}Cl_4$ 2.253 (3)	$Cl_4\text{-}Zn\text{-}Cl_2$ 111.16 (1)
$Zn\text{-}Cl_5$ 2.230 (4)	$Cl_5\text{-}Zn\text{-}Cl_2$ 110.26 (1)
	$Cl_5\text{-}Zn\text{-}Cl_3$ 107.60 (1)
	$Cl_5\text{-}Zn\text{-}Cl_4$ 109.71(1)

The organic part is formed by two types of organic chains $(C_6H_5\text{-}C_2H_4\text{-}NH_3)^+$ (1) and $(C_6H_5\text{-}C_2H_4\text{-}NH_3)^+$ (2). The torsion angles NCCC are 178.76° and 175.65° for chains (1) and (2) respectively indicate the planarity of the cations. Overall the crystal structure cohesion is obtained via various types of interactions. The principal feature of interest in these structures is hydrogen bonding (Figure 3) that significantly contributes in the stabilization of the crystal structure. Each chlorine atoms contributes in three hydrogen bonding, the length of this bond d (Ni·····Clk) is in the ranges of 3.314 to 3.448 Å (Table 4). The presence of π-π stacking interactions between phenyl rings presents another kind of interactions. The measurement of their forces is determinate by the centroids distance between neighboring phenyl ring d (4.663 Å) and the two angles (α, α0); (61.64°, 7.71°) between the normal of each mean plane through these rings and the centroid-centroid axis, that demonstrates the presence of a weak π-π stacking.

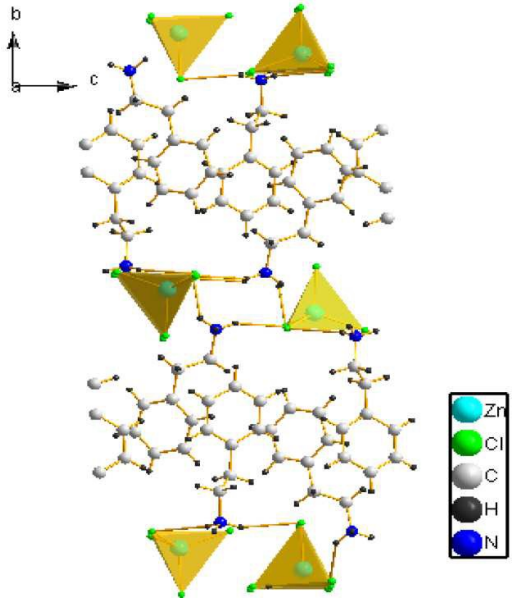

Fig. 2 Overall view of the crystal packing along the a-axis

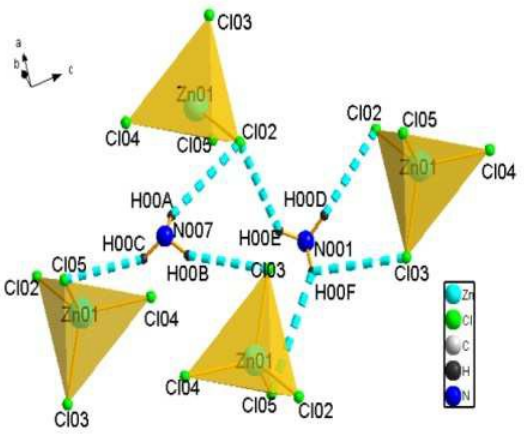

Fig. 3 Scheme of Hydrogen-bonding interactions in PEA-$ZnCl_4$

Table 4 Hydrogen bonding parameters in PEA-$ZnCl_4$

N-H ···· Cl (°)	N ···· Cl (Å)
163.98 (2)	3.294 (1)
126.66 (2)	3.321 (1)
158.33 (2)	3.382 (1)
149.40 (2)	3.321 (1)
112.37 (3)	3.396 (2)
127.39 (2)	3.448 (1)

For obtaining a perfectly packed system the quantification of the cation sizes was calculated by tolerance factor traditionally gives by Gold Schmitt et al [35] and extended for organic-inorganic by Kieslich et al [36], by applying the following equation:

$$\alpha = \frac{\left(r_{Aeff} + r_{Xeff}\right)}{\sqrt{2}\left(r_B + 0.5h_{Xeff}\right)}$$

Where r refers to the effective molecular or ionic radius of the A-site, B-site and X anionic-site while h_{Xeff} refers to the height of the anions in the direction between B-site cations. The obtained value (α=1.17) is larger than that calculated for $[NH_4]Cd(HCOOH)_3$ (α =0.62) [37] and $RbMnIJHCO_2)_3$ (α =0.66) [38] and nearly of that obtained for hydrated methyl ammonium cation ($[CH_3NH_3.H2O]$ (α =1.13) [39] . This value is broad as than 1 and is a feature of layered organic inorganic [40].

Thermal analysis

The Thermogravimetric analysis (TGA) was carried out to characterize the thermal stability, which was presented in Figure 4. It's found that the simple is stable below 541 K (temperature of decomposition), but decomposes over that point, the weight loss transition has an onset at about 541 K and a corresponding mass loss of 65.24%, almost consistent with the predicted value of 69.82 % for the dissociation of $(C_6H_5\text{-}C_2H_4\text{-}NH_3)_2,2Cl$.

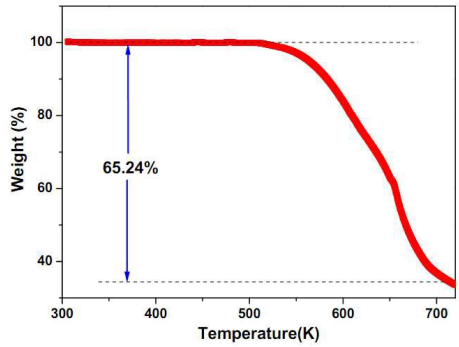

Fig. 4 TGA curve of PEA-ZnCl4

In order to investigate the phase transitions and the enthalpy for the PEA-$ZnCl_4$, Differential Scanning Calorimetry (DSC) was carried out (Figure 5). It is observed that the compound is stable up to 541 K (melting temperature), and exhibits two first order phase transitions. An overview of the results obviously shows the existence of two endothermic peaks clearly seen at 464 K and at 501 K on heating. Moreover, two exothermic peaks shows at 485 K and at 452 K on cooling. The temperature hysteresis of the peaks at 464 K and 501 K were observed to be 12 and 16 K, respectively. These peaks are associated with a reversible phase transition in the PEA-ZnCl4 crystals. This transition probably proof of order-disorder transition of alkyl ammonium [41, 42]. The transition enthalpies ΔH and entropies ΔS with the peaks temperature on heating and cooling are presented in Table 5. There are no significant differences in the enthalpy and entropy values between the corresponding peaks in cooling or warming modes.

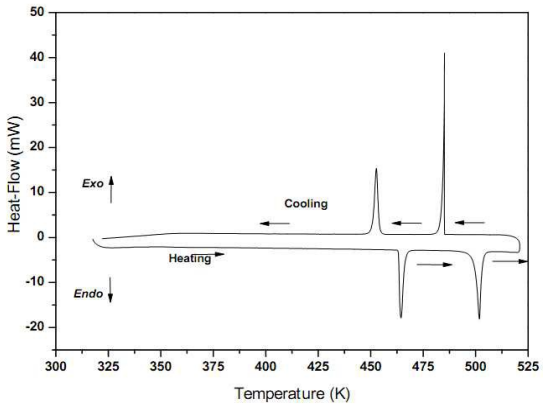

Fig. 5 DSC thermograph of PEA-$ZnCl_4$

Table 5 Calorimetric values from DSC measurements for PEA-$ZnCl_4$

	Heating	Cooling
T (K)	464 ; 501	452 ; 485
ΔH ($J.g^{-1}$)	40.74 ; 49.74	39.63 ; 47.89
ΔS ($J.K^{-1}.mol^{-1}$)	39.64 ; 44.83	39.59 ; 44.58

Optical band gap

The UV-vis diffuse reflectance spectrum measured and absorption spectrum calculated for PEA-$ZnCl_4$ are represented in Figure 6. They show an absorption edge of about 278 nm and the missing absorption in the wavelengths upper than 450 nm. We can in particular note the presence of a direct band energy transition. We have also determined the band gap by fixing the tangent line of the curve and the energy axis. This obtained value is approximately of 4.46 eV characteristic of an insulator material.

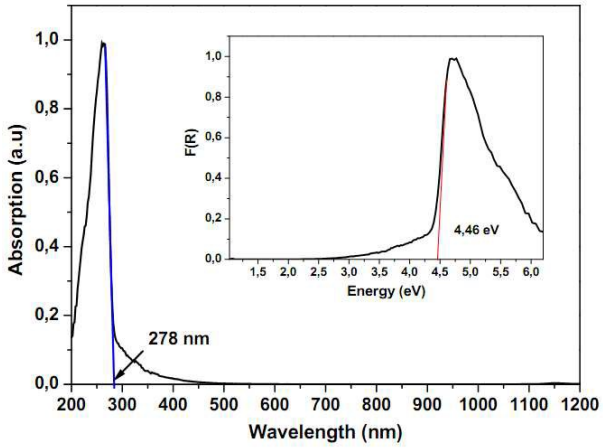

Fig. 6 UV-vis diffuse reflectance plots for PEA-$ZnCl_4$

Electronic properties

The calculated electronic band structure of PEA-$ZnCl_4$ compound is shown in Figure 6a. The analysis of different direction, reveal the missing of energy dispersion along the (Γ-Y) direction (equivalent to the staking axis in real space), there is an ingrained consequence of dielectric mismatch between inorganic and organic layers [43]. The small dispersion observed along (Y-A), (A-R), (R-D) and (D-A) directions (Figure 6b) may be coming from the reduced dielectric mismatch between sheets and a weak coupling between inorganic layers [44]. Furthermore, the band structures disclose a direct band-gap transition located at the Γ point. The calculated band gap energy is of about 4.36 eV, this value is slightly smaller in comparison to the experimental band gap value (4.46 eV). These results explained by the underestimation supported by ground state DFT computations.

The composition of the calculated bands can be deduced from the analysis of the partial density of states (PDOS) and total density of states (DOS) diagrams shown in Figure 8. The lowest part of the valence band (VB) consists of nitrogen 2s orbitals located at -21 eV, whereas the chlorine 3s located at -13 eV. The range energy of -12.5 to -5 eV is the feature of the mixed contribution between carbon (2s, 2p orbitals), nitrogen (2p orbital) and hydrogen. We can attribute this result to the electronic cloud around N-H and C-H bands. While the maximum of the valence band (MVB) is composed by the mixed states 3d of zinc, 3p of chlorine and 2p of carbon. The minimum of the conduction band (MCB) consists of orbital 3s of zinc, 3p of chlorine and 2p of carbon. Note that the results are different from those found for $CH_3NH_3PbI_3$ [45, 46], wherein the responsible orbital in MVB and MCB are s and p orbitals for iodine and lead atoms. The 3D gap analysis by Xcrysden [47] extracted from the calculated density (Figure 9) show the existence of empty spaces, corresponding to the interactions between different aggregates. The result is in good agreement with that obtained by X-ray diffraction and the density of states. This, confirm the role of hydrogen binding (Figure 9b) in crystal structure building and the insulation between the tetrahedra. Also, the presence of a weak π-π stacking between organic fragments (Figure 9c).

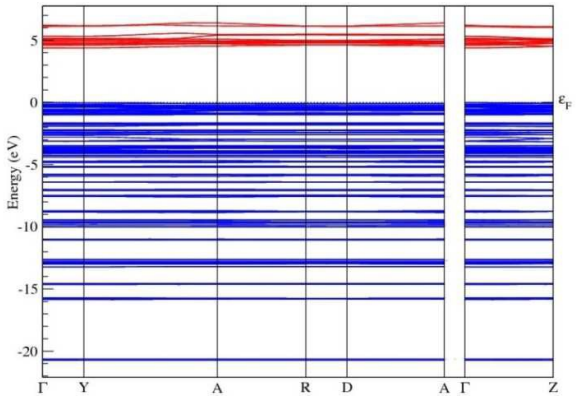

(a)

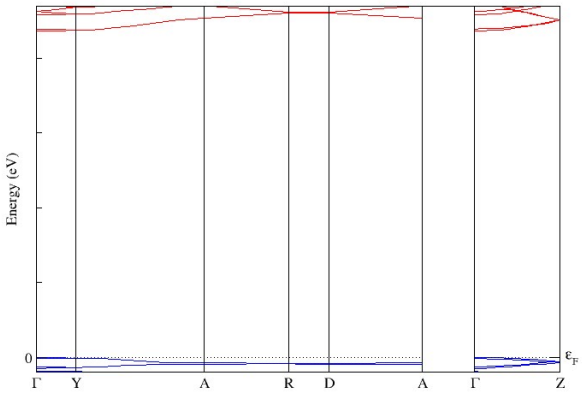

(b)

Fig. 7 (a) Band structure calculated of PEA-$ZnCl_4$, **(b)** Dispersed energy between MVB and MCB

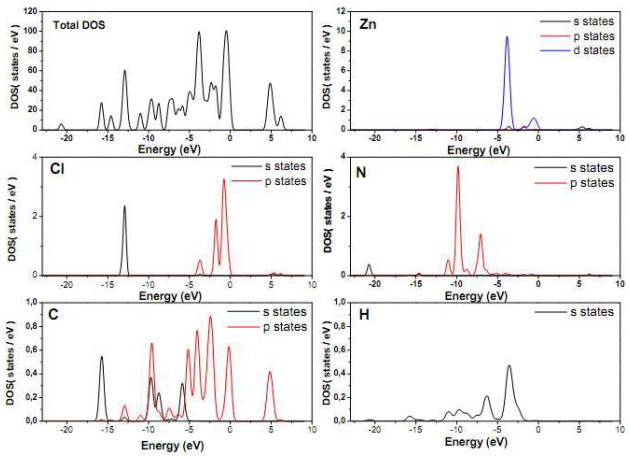

Fig. 8 Calculated DOS and PDOS diagrams for PEA-ZnCl4

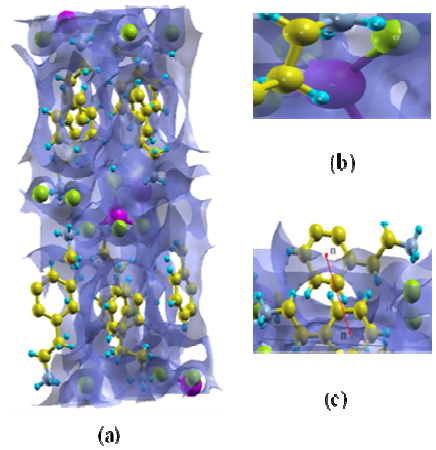

Fig. 9 Calculated 3D Gap Density: **(a)** Overall Crystal, **(b)** Hydrogen bond, **(c)** π-π stacking between phenyl rings

Conclusions

The organic-inorganic hybrid perovskite, (C6H5-C2H4-NH3)2ZnCl4 has been synthesized and crystallized successfully by diffusion method. The single crystal X-ray diffraction investigation at 293 K confirms the formation of 0D organic-inorganic hybrid structure. The TGA analysis reveals that this compound is stable below 541 K. Two reversible phase transitions have been shown by Differential Scanning Calorimetry measurements. The UV-visible reflectance measurements reveal that the compound present a direct band gap transition with gap energy about 4.46 eV, characteristic of an insulator material. The calculated band gap energy obtained by DFT is in good agreement with experimental band gap value. The density calculations allowed us to demonstrate clearly the density dispersion in the first Brillouin Zone.

Acknowledgements

This work has been initiated with the support of URAC08, Project RS: 02 (CNRST). We thank also Prof. S. Aït Lyazidi and Prof. M. Haddad, LASMAR Laboratory, Moulay Ismail Univ. Morocco, for recording optical measurements.

References

1 D. B. Mitzi, Prog. Inorg. Chem, 2007, **48**, 1-121.
2 S. Zhang, G Lanty, J. S. Lauret, E. Deleporte, P. Audebert and L. Galmiche, Acta. Mater, 2009, **57**, 3301-3309.
3 D. Ionescu, I. Ciobanu and I. Radinschi, J. Optoelectron. Adv. M, 2007, **9**, 2608-2616.
4 S. Zhang, P. Audebert, Y. Wei, J. S. Lauret; L. Galmiche and E. Deleporte, J. Mater. Chem, 2010, **21**, 466-474.
5 M. Mostafa and S El-Khiyami, J. Solid. State. Chem, 2014, **209**, 82-88.
6 B. Kulicka, R. Jakubas, Z. Ciunik, G. Bator, W. Medycki, J. Świergiel and J Baran, J. Phys. Chem. Solids, 2004, **65**, 871-879.
7 C. B. Mohamed, K. Karoui, S. Saidi, K. Guidara and A. B Rhaiem, Physica B, 2014, **451**, 87–95.
8 S. Kalyanaraman, P. Shajinshinu and S. Vijayalakshmi, J. Phys. Chem. Solids, 2015, **86**, 108–113.
9 T. Baikie, Y. Fang, j. M. Kadro, M. Schreyer, F. Wei, S. G. Mhaisalkar, M. Graetzel and T. J. White, J. Mater. Chem, 2013, **A1**, 5628-5641.
10 Nicole A. Benedek, James M. Rondinelli, Hania Djani, Philippe Ghosezd and Philip Lightfoote, Dalton. Trans, 2015, **44**, 10543-10558.
11 Ziyong Cheng and Jun Lin, CrystEngComm, 2010, **12**, 2646-2662.
12 C. Kagan, D. B. Mitzi and C. Dimitrakopoulos, Science, 1999, **286**, 945–947.
13 C. Zhang, D. Sun, C. X. Sheng, Y.X. Zhai, K. Mielczarek, A. Zakhidov and Z. V. Vardeny, Nat. Phys, 2015, 11, 427-434.
14 Q. Chen, N. De Marco, Y. M. Yang, T-B. Song, C-C. Chen, H. Zhao, Z. Hong, H. Zhou and Y. Yang, NanoToday, 2015, **10,** 355-396.
15 D. B. Mitzi, K. Chondroudis and C. R. Kagan, IBM Journal of Research and Development, 2001, **45**, 29-45.
16 D. B. Mitzi, Dalton. Trans, 2001, **1**, 1-12.
17 J. L. Knutson, J. D. Martin and D. B. Mitzi, Inorg. Chem, 2005, **44**, 4699-4705.
18 D. B. Mitzi, Chem. Mater, 2001, **13**, 3283-3298.
19 M. F. Mostafa, S. S. El-Khiyami, 2014, *Journal of Solid State Chemistry*, ***209***, 82-88.
20 M. Ben Bechir, K. Karoui, M. Tabellout, K. Guidara, A. Ben Rhaiem, 2014,, J. Appl. Phys,115, 153708
21 M. M. Abdel-kader, A. I. Aboud, W. M. Gamal, 2015, Phase Transitions, 1-23
22 E. A. Buvaylo, V. N. Kokozay, R. P. Linnik, O. Y. Vassilyeva, B. W. Skelton, 2015,.Dalton Transactions,44, 13735-13744
23 A. Altomare, M. Burla, M. Camalli, G. Cascarano, C. Giacovazzo, A. Guagliardi, A. Moliterni, G. Polidori and R. Spagna, J. Appl. Cryst, 1999, **32**, 115-119.
24 M. Sheldrick, Acta Cryst, 2007, **A64**, 112-122.
25 L. Farrugia, J. Appl. Cryst, 1999, **32**, 837-838.
26 Brandenburg K, Crystal Impact GbR, (2010), Bonn, Germany.
27 M. Butler, J. Appl. Phys, 1977, **48**, 1914-1920.
28 W. Kohn and L. Sham, J. Phys. Rev, 1965, **A140**, 1133-1138.
29 J. Perdew, K. Burke and M. Ernzerhof, Erratum Phys. Rev. Lett , 1997, **78**, 1396.
30 X. Gonze, J-M. Beuken, R. Caracas, F. Detraux, M. Fuchs, G-M. Rignanese, L. Sindic, M. Verstraete, G. Zerah, F. Jollet, M. Torrent, A. Roy, M. Mikami, Ph. Ghosez, J.-Y. Raty and D. C. Allan, Comp. Mater. Sci, 2002, **25**, 478-492.

31 H. J. Monkhorst and J. D. Pack, Phys. Rev, 1976, **B13**, 5188.
32 Y-D. Huh, J. H. Kim, S. S. Kweon, W-K. Kuk, C-S. Hwang, J-W. Hyun, Y-J. Kim and Y. Park, Curr. Appl. Phys, 2006, **6**, 219-223.
33 W. Baur, Acta. Cryst, 1974, **B30**, 1195-1215.
34 M. A. Fersi, I. Chaabane, M. Gargouri and A. Bulou, Polyhedron, 2015, **85**, 41-47.
35 V. M. Goldschmidt, Naturwissenschaften, 1926, 14, 477–485.
36 G. Kieslich, S. Sun and A. K. Cheetham, Chem. Sci., 2014, 5, 4712–4715.
37 L. C. Gómez-Aguirre, B. Pato-Doldán, A. Stroppa, S. Yáñez-Vilar, L. Bayarjargal, B Winkler, S. Castro-García, J. Mira, M. Sánchez-Andújar, and M. A. Señarís-Rodríguez, Inorg.Chem., 2015, **54**, 2109–2116
38 S M. Bovill and P J. Saines, CrystEngComm, 2015, **17**, 8319-8326.
39 G. H. Imler, X. Li, B. Xu, G. E Dobereiner, H. L. Dai, Y. Rao, B. B. Wayland, Chemical Communications, 2015, **51**, 11290-11292.
40 D. B. Mitzi, Journal of the Chemical Society, Dalton Transactions, 2001, **1**, 1-12.
41 T. Yoshinari, T. Nanba, S. Shimanuki, M. Fujisawa and K. Aoyagi, J. Phys. Soc. Jpn, 1992, **61**, 2224-2226.
42 D. B. Mitzi, Chem. Mater, 1996, **8**, 791-800.
43 J. Even, L. Pedesseau, M-A. Dupertuis, J-M. Jancu and C Katan, Phys. Rev, 2012, **B86**, 205301.
44 Y. Wang, T. Gould, J. F. Dobson, H. Zhang; H. Yang, X. Yao and H. Zhao, Phys. Chem. Chem. Phys, 2014, **16**, 1424-1429.
45 L. Pedesseau, J-M. Jancu, A. Rolland, E. Deleporte, C. Katan and J. Even, Opt. Quant. Electron, 2014, **46**, 1225–1232.
46 J. Navas, A. Sanchez-Coronilla, J. J. Gallardo, N. Cruz Hernandez, J. C. Pinero, R. Alcantara, C. Fernandez-Lorenzo, D. M. De los Santos, T. Aguilar and J. Martin-Calleja, Nanoscale, 2015, **7**, 6216-6229.
47 A. Kokalj, Journal of Molecular Graphics and Modelling, 1999, **17**, 176-179.